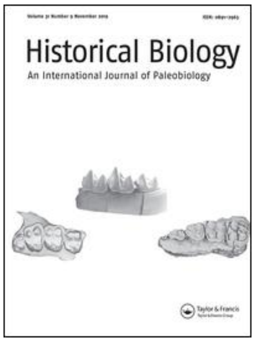

Taylor & Francis
Taylor & Francis Group

Historical Biology

An International Journal of Paleobiology

ISSN: 0891-2963 (Print) 1029-2381 (Online) Journal homepage: https://www.tandfonline.com/loi/ghbi20

Internal morphology of nasal spine of *Tsintaosaurus spinorhinus* (Ornithischia: Lambeosaurinae) from the upper cretaceous of Shandong, China

Jialiang Zhang, Xiaolin Wang, Shunxing Jiang & Guobiao Li

HISTORICAL BIOLOGY
https://doi.org/10.1080/08912963.2020.1731804

Taylor & Francis
Taylor & Francis Group

ARTICLE

Internal morphology of nasal spine of *Tsintaosaurus spinorhinus* (Ornithischia: Lambeosaurinae) from the upper cretaceous of Shandong, China

Jialiang Zhang[a,b], Xiaolin Wang[a,c,d], Shunxing Jiang[a,c] and Guobiao Li[b]

[a]Key Laboratory of Vertebrate Evolution and Human Origins of Chinese Academy of Sciences, Institute of Vertebrate Paleontology and Paleoanthropology, Chinese Academy of Sciences, Beijing, China; [b]School of the Earth Sciences and Resources, China University of Geosciences (Beijing), Beijing, China; [c]CAS Center for Excellence in Life and Paleoenvironment, Beijing, China; [d]College of Earth and Planetary Sciences, University of Chinese Academy of Sciences, Beijing, China

ABSTRACT

Tsintaosaurus spinorhinus is famous for the unique rod-like nasal spine, but there has been a long debate about whether its nasal spine is hollow, since it is difficult to examine the nasal inside through direct observation. Here, we used a high-resolution CT scan to reveal the interior structure of the nasal spine and re-observed the holotype and paratype of *Tsintaosaurus spinorhinus*. By the direct observation and CT scan, we provide new information about the nasal spine of *Tsintaosaurus spinorhinus*, and our result shows the rod-like nasal spine of *Tsintaosaurus spinorhinus* is a solid sandwich structure, rather than a hollow tubular structure. There is a significant fracture between the rod-like process and the base of the nasal, and if the two processes fit together, the nasal spine would have been more inclined rostrally in life. The new cranial information collected through the direct observation and CT scan reveals that the narrow strip surrounded by the nasals and frontals is formed by a longitudinal median groove filled with sediment, indicating the possible presence of the frontal-nasal fontanelle in younger juveniles.

ARTICLE HISTORY
Received 13 November 2019
Accepted 16 February 2020

KEYWORDS
Lambeosaurinae; *Tsintaosaurus*; computed tomography scan; upper cretaceous; China

Introduction

Lambeosaurine dinosaurs are among the most diverse and abundant ornithopod dinosaurs that lived during the Late Cretaceous (Horner et al. 2004; Prieto-márquez 2010a). Lambeosaurine is characterised by hypertrophied nasal passages associated with a wide shape variety of hollow supracranial crests (Horner et al. 2004; Prieto-márquez 2010a). The predominant function of these crests might be species recognition and sexual display (Hopson 1975; Evans 2006). Lambeosaurines were widely distributed during Santonian to Maastrichtian of Late Cretaceous, and their fossil remains have been found in Asia, Europe, North and South America (Lund and Gates 2006; Prieto-márquez 2010b). Indeed, many fossil Lambeosaurine hadrosaurids have been found in Asia (Nagao 1936; Riabinin 1938; Young 1958; Rozhdestvensky 1968; Bolotsky and Kurzanov 1991; Godefroit et al. 2000, 2003, 2008; Lund and Gates 2006; Prieto-márquez 2010b; Bell and Brink 2013).

Tsintaosaurus spinorhinus (Young 1958), one of the well-known Asian lambeosaurine, was recovered from the red beds of the Jingangkou Formations of Upper Cretaceous, Wangshi Groupin the Laiyang basin, Shandong, eastern China (Wang et al. 2010; Prieto-Márquez and Wagner 2013; Zhang et al. 2017a), and the age of the exposed fossil layers was interpreted as late Campanian to early Maastrichtian of the Late Cretaceous (Yan and Chen 2005; Liu et al. 2010; Xing et al. 2014; An et al. 2016). The Wangshi Group in the Laiyang basin has yielded a variety of dinosaur groups, including Hadrosauroidea (Wiman 1929; Young 1958; Hu 1973; Zhen 1976; Zhang et al. 2017b, 2019), Ankylosauridae (Buffettaut and Tong 1995), Pachycephalosauridae (Dong 1978), Theropoda (Young 1958; Poropat and Kear 2013), Stegosauria (Young 1958), and Sauropoda (Young 1958). This dinosaur assemblage was referred to the Laiyang Hadrosauroid Fauna, one of the most important and famous Late Cretaceous dinosaur faunas in China (Wang et al. 2010; Zhang et al. 2017a).

Young (1958) described *Tsintaosaurus spinorhinus* based on a nearly complete composite skeleton (IVPP V 725), an incomplete skull (IVPP V 818), and additional postcranial materials from a small gully near the Jingangkou Village, Laiyang. *Tsintaosaurus spinorhinus* has a rod-like, anterodorsally projected cranial crest, formed by the nasals (Figure 1). Because this extraordinary structure differs from the crest of other lambeosaurines, which incorporate both the nasals and the premaxillae (Ostrom 1962; Hopson 1975; Horner et al. 2004; Evans et al. 2009), some scholars questioned whether the nasal spine was hollow and the validity of the taxon (Rozhdestvensky 1968, 1977; Horner and Weishampel 1990; Taquet 1991). However, some researchers believed that *Tsintaosaurus spinorhinus* was assignable to Lambeosaurinae and most likely had a hollow crest, based on the presence of lambeosaurine features in the skull and postcranial bones (Maryańska and Osmólska 1981; Brett-Surman 1989; Buffettaut and Tong 1993, 1995; Horner et al. 2004). Prieto-Márquez and Wagner (2013) reconstructed the cranial crest of *Tsintaosaurus spinorhinus* as a hollow posterodorsally projected structure as in typical lambeosaurines, based on the morphology and bone contact relationships of the holotype and paratype skulls (IVPP V 725 and IVPP V 818) and an additional fragment of the crest bone (IVPP V 829). They also questioned whether the nasal is a hollow tube, since the cross-sectional area of the tubular process of the nasals is relatively small and there is no ventral exit to the intracranial space (Prieto-Márquez and Wagner 2013), which contradicts Young's (1958) original description.

In recent years, the computed tomography (CT) scan and the visualisation software have been generally used for non-destructive reconstruction of digital endocast and other intraosseous structures of hadrosaurids (Sullivan and Williamson 1999; Bell et al. 2009; Evans et al. 2009; Godefroit et al. 2012; Farke et al. 2013; Lauters et al. 2013; Cruzado-Caballero et al. 2015; Ramírez-Velasco et al. 2017; Becerra et al. 2018). These non-invasive techniques could reveal the internal anatomy of the lambeosaurine crest as a digital visualisation model

CONTACT Xiaolin Wang wangxiaolin@ivpp.ac.cn Key Laboratory of Vertebrate Evolution and Human Origins of Chinese Academy of Sciences, Institute of Vertebrate Paleontology and Paleoanthropology, Chinese Academy of Sciences, Beijing 100044, China

Published online 19 Mar 2020

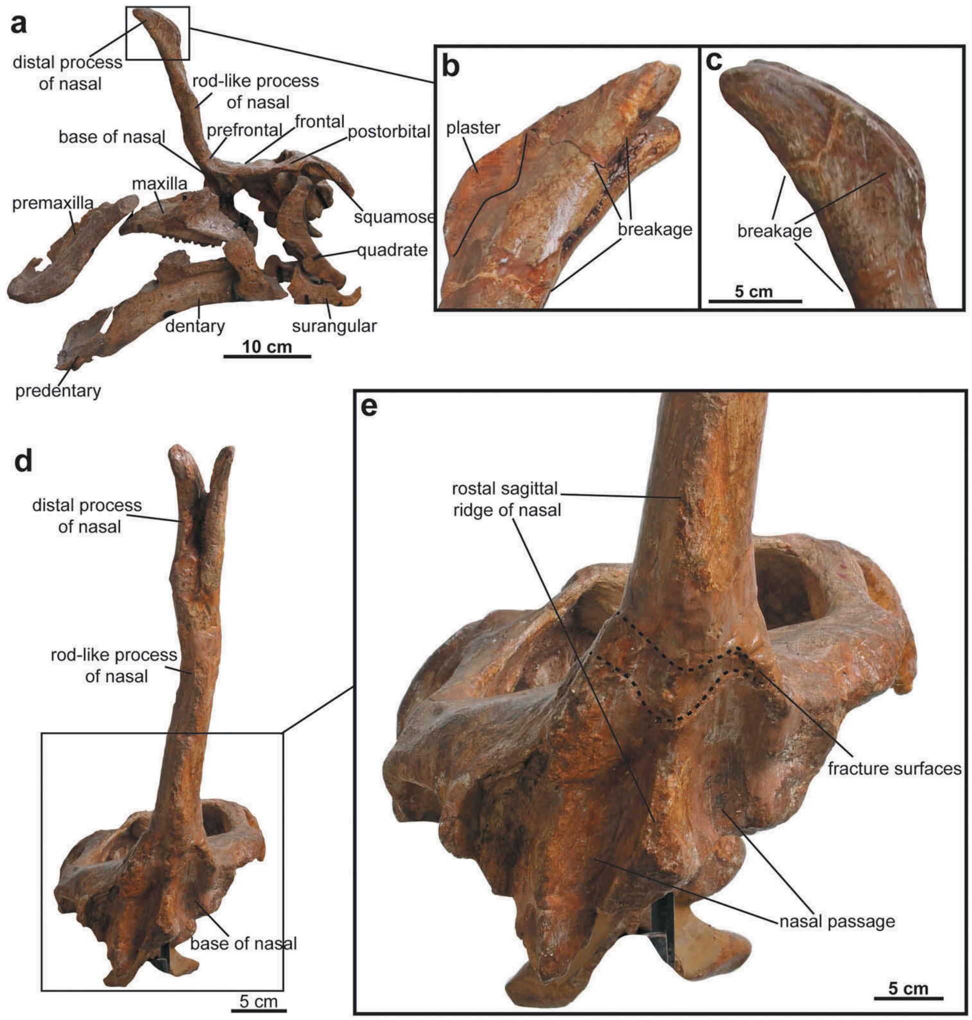

Figure 1. Nasal of *Tsintaosaurus spinorhinus* (IVPP V 725). Skull of *Tsintaosaurus spinorhinus* (IVPP V 725) in left lateral (a) and rostral (d) views. Distal process of the nasal in right (b) and left (c) lateral views. Ventral part of the nasal in rostral view (e), the fracture surface between the rod-like process and the base of nasal marked by dotted lines.

(Sullivan and Williamson 1999; Evans et al. 2009; Farke et al. 2013). Here we re-examined the skull of *Tsintaosaurus spinorhinus* and scanned the spine of *Tsintaosaurus* (IVPP V 725) with a CT scanner and reconstructed its internal structure.

Institutional abbreviations

IVPP: Institute of Vertebrate Paleontology and Paleoanthropology, Chinese Academy of Sciences.

Materials and methods

Fossil specimen

The specimens studied herein, are the crania of the holotype (IVPP V 725) and paratype (IVPP V 818) of *Tsintaosaurus spinorhinus*, which were collected from the same site located in western of Jingangkou Village, Laiyang City, Shandong Province, and all are housed in the Institute of Vertebrate Paleontology and Paleoanthropology, Chinese Academy of Sciences, Beijing, China.

CT scanning

The crest of the holotype of *Tsintaosaurus spinorhinus* (IVPP V 725) was scanned with 450 ICT scanner with a voltage of 400 kV and a current of 150 mA at the Key Laboratory of Vertebrate Evolution and Human Origins of Chinese Academy of Sciences. The inter-slice spacing was 0.5 mm, and a total of 800 transmission images were captured for each sample, each image being 2048*2048 pixels. The scan data were imported to the volume analysis software VGStudio Max 2.1 (Volume Graphics, Germany), and were then transferred into Mimics 16.0 (Materialise, Belgium) for segmentation, visualisation, and analysis.

Results

Nasal spine external description

Only in the holotype, IVPP V 725, the nasals are almost completely preserved, and fuse sagittal to form a rod-like, anterodorsally projected nasal spine (Figure 1(a,d), 2(a,b)). The paired nasals form a thick median ridge along the rostral of the midline suture and a shallow groove along the caudal surface (Figures 1(d), 2(a,b)). There is a slope on each lateral side of the rod-like process between the wide caudal surface and narrow rostral surface, thus forming a heart-shape cross section.

The rod-like process terminates in two branches dorsally, which form the thin distal process with fan-shaped and rostrocaudally expanded lateral profile (Figure 1(b,c)). However, both of the two

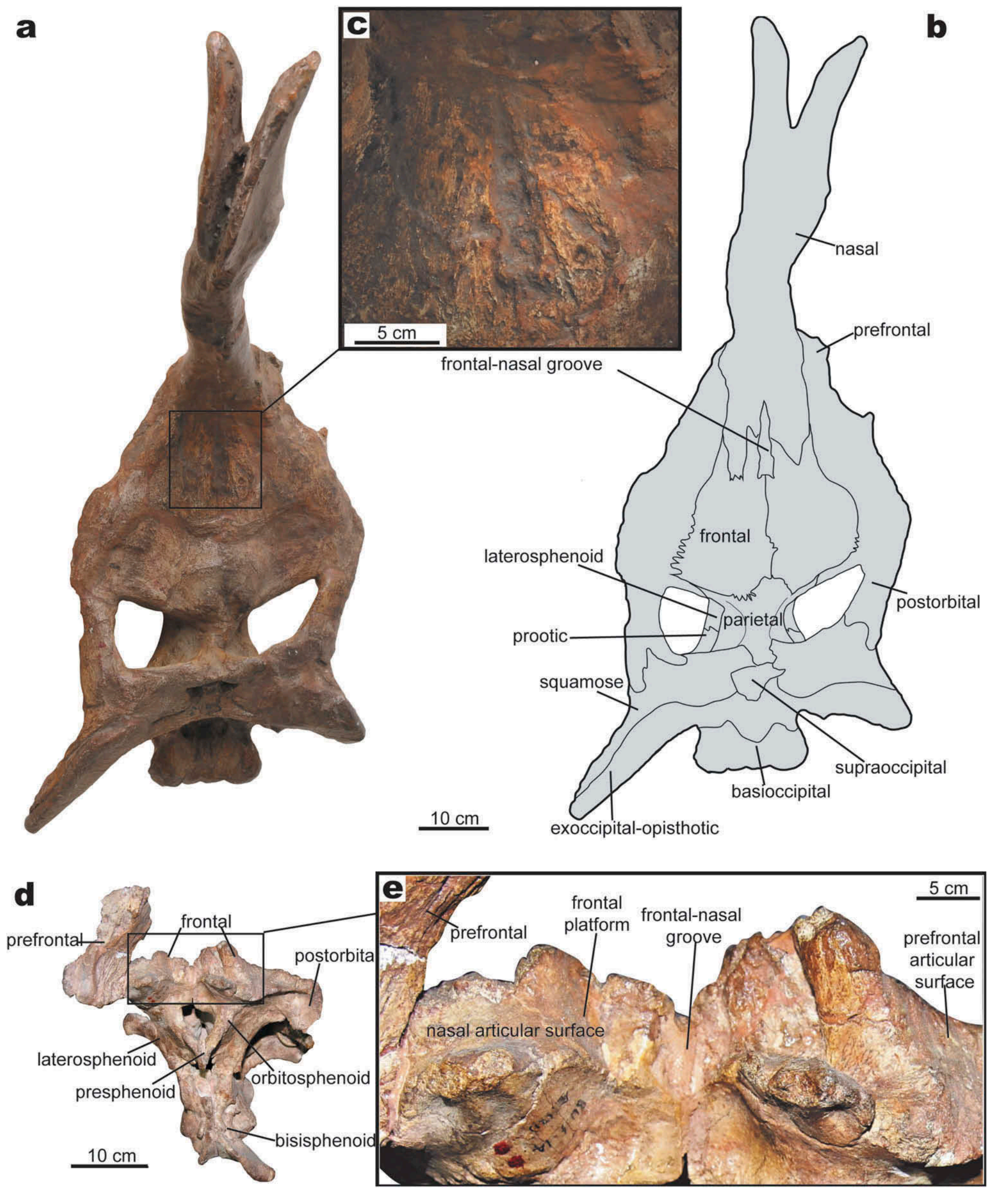

Figure 2. Frontal-nasal groove of *Tsintaosaurus spinorhinus*. Holotype skull of *Tsintaosaurus spinorhinus* (IVPP V 725) in dorsal view (a). Line drawing of the same skull in dorsal view (b). Frontal-nasal groove in dorsal view (c), narrow shallow strip structure surrounded by nasals and frontals, interpreted as the frontal-nasal groove filled with sediment. Paratype skull of *Tsintaosaurus spinorhinus* (IVPP V 818) in rostral view (d). Nasal articular surface of frontal in rostral view (e), deep cleft between the two nasal articulate surfaces interpreted as the frontal-nasal groove.

distal processes were mutilated when the fossil was collected, and the breakage was restored by plaster as described by Young (1958) (Figure 1(b)).

At the base of the nasal spine, the nasals extend ventrally to form the rostrodorsal part of the neurocranium, which is surrounded by the upturned portions of frontal caudally and prefrontal laterally (Figure 1(d,e)). In the rostral view, the block-like process tapers dorsally into the rod-like nasal spine. The rostral sutures between the nasal and prefrontal form two narrow dorsoventrally oriented ridges, which cooperate with the middle ridge to separate the rostral face of the block into two concave passages (Figure 1(e)). The passages shallow dorsally and end at the level of the dorsal margin of the prefrontal, and two elliptical depressions locate in the rostral surface of the passages of the base of the nasal. It is possible that the middle ridge of the block would connect into the middle ridge of the rod-like process, although there is a significant fracture between the two parts of the nasal.

In dorsal view, the caudal portion of the nasal contacts the frontal by a highly interdigitate suture (Figure 2(a,b)), and divides into two branches by the narrow strip structure, which is slightly concave and bordered by a thin ridge with surround nasal and frontal (Figure 2(c)). The material in this strip structure is more similar to that in suture rather than the material of the nasal and frontal bones. In addition, in the paratype, IVPP V 818, the nasal is not preserved, and the nasofrontal contact is exposed (Figure 2(d)). There is no evidence of the rostromedial process, but a deep cleft between the two nasal articulate surfaces of the frontals (Figure 2(e)). We speculate that the narrow strip-like structure is equivalent to the deep cleft in IVPP V 818, which is filled with sediment. Thus, this structure would be not the rostromedial process of frontal as the description of Prieto-Márquez and Wagner (2013), but a narrow groove opening between the nasal and frontal bones.

Nasal spine internal description

The CT scan of the nasal shows that two distal processes are mostly less denser and are interpreted as fractures, repaired with artificial materials such as plaster (Figure 3(d-h)). Particularly, the terminal of the left distal process is entirely artificial (Figure 3(d)). In the main body of the distal process, the bones are found at the rostral portion of the right branch and the caudal portion of the left branch, and exhibit a progressive increase in thickness and length towards the basal portion of the distal process. The CT scan reveals three layers in the left distal process, a dense layer is sandwiched between two less dense layers (Figure 3(f-h)). However, only two layers are observed in the right branch, a denser part in the medial and a less denser part in the cortical region. The missing layer may be caused by erosion. Additionally, there is an obvious breakage on the rostral surface of the right branch (Figure 3(e-g)). This observation is compatible with the external description, confirming the interpretation of Prieto-Márquez and Wagner (2013) regarding the distal nasal process of IVPP V 725 as the incomplete caudodorsal half of the rhomboid structure preserved in IVPP V 829 (figure 2 (a,c) in Prieto-Márquez and Wagner 2013). At the base of the distal process, a grey strip-like area is located between the two branches (Figure 3(f,g)), which may be interpreted as the sediment and glue, confirming the external observation The grey strip-like area gradually decreases in thickness ventrally and becomes a vein as the two branches of the distal process converge into the rod-like process of the nasal spine (Figure 3(i)). At the connection between the distal process and rod-like process, there is a severe post-depositional fracture, which is visible after the 3D reconstruction of the CT scan (Figure 3(a)).

The CT scan reveals a sandwich structure in the main body of the nasal spine (Figure 3(i–m)), which has the same structure as the left distal process. In our three-dimensional reconstruction, there is a long strip in the middle along the sagittal plane, this structure is interpreted as the rectangular medial dense part of the cross section (Figure 3(a)). In most of the main body of the nasal, the middle part

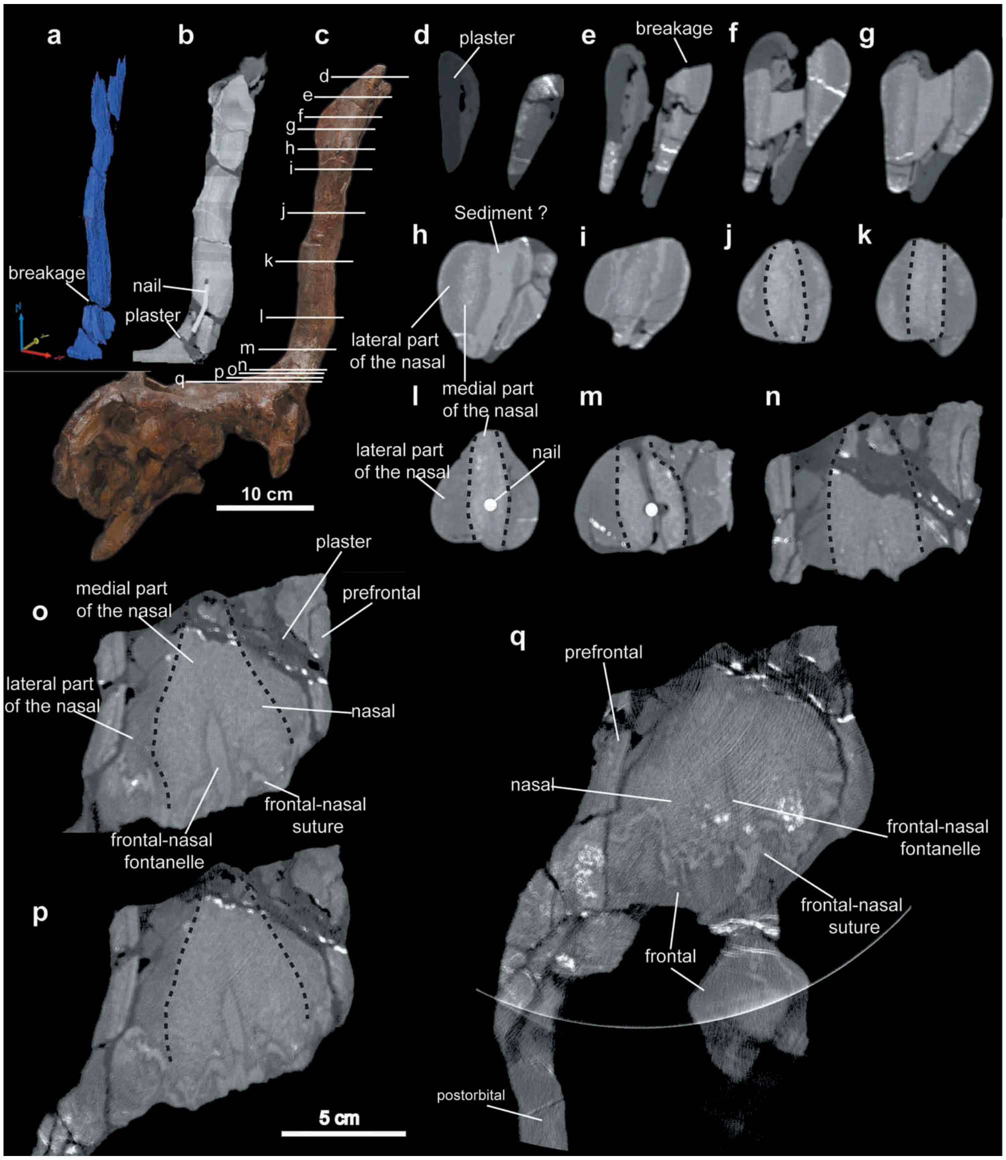

Figure 3. CT scan images of the nasal spine of *Tsintaosaurus spinorhinus* (IVPP V 725). 3D reconstruction of the medial part of the nasal (a). CT scan image of sagittal section of the nasal (b). Braincase with nasal in right lateral view (c), illustrating the relative locations of the cross sections (d–q). CT scan images of the distal process of the nasal in different cross sections (d–h). CT scan images of the rod-like process of the nasal in different cross sections (i–m), the medial part of the nasal marked by dotted lines. CT scan images of the base of the nasal in different cross sections (n–q), the medial part of the nasal marked by dotted lines.

extends throughout the whole cross section of the nasal, from the rostral to caudal surface. Although the fractures destroyed the borders in several portions of the nasal, we still observed that the rostral margin of the middle part fused into the rostral surface of the rod-like process. In addition, the caudal margin of the nasal base coincides with the caudal surface of the nasal spine. Therefore, instead of forming a cavity around the middle, the two lateral parts sandwich the middle between them. As a consequence, the crest of *Tsintaosaurus* could not enclose a nasal cavity, which is divided into a pair of hollow passage in the crest of all the other lambeosaurines. In addition, the middle part of the crest of *Tsintaosaurus* is also part of the skeleton, and the crest would be solid, not hollow.

As the rod-like process descends ventrally into the base of the nasal, there is a lower density region interpreted as lateral part of the nasal and a dense area interpreted as prefrontal in each lateral side of the middle part of the nasal (Figure 3(n-q)). The middle dense part of the nasal increases wider and forms a heart shape in cross section, with a rostral taper is interpreted as the middle ridge of the nasal base, while the caudal margin of the middle part articulates with the upturned rostral process of the frontal. Between the nasal and frontal, there is a zigzag higher density line interpreted as the nasal-frontal suture (Figure 3(o-q)). The CT scan of the nasal base reveals a fusiform denser area that locates between the two branches of the caudal process of the nasal and separates with the rostral processes of the frontals (Figure 3(n-q)). The density has obvious distinction between the fusiform area and the medial part of the nasal, the former is more homogeneous. The fusiform denser area, increasing in size towards the dorsal surface of the braincase, connects to the nasal-frontal suture in the layers closed the braincase. This observation is compatible with the external description above, and this area is interpreted as a narrow groove.

Discussion

Our study concurs with Buffettaut and Tong (1993, 1995) that *Tsintaosaurus spinorhinus* should be assignable to Lambeosaurinae. *Tsintaosaurus spinorhinus* exhibits a series of characteristics of Lambeosaurinae (Horner et al. 2004; Prieto-márquez 2010a), including the frontal being completely excluded from the orbital margin, the upward doming on the dorsal part of the frontal, the width being greater than the length of the supratemporal fenestra, the parietal sagittal crest being relatively short and down-curved, the anterodorsal process absent in the anterior of the maxilla, the dorsal process of the maxilla being posterodorsally extended, the symphyseal process of the dentary being medioventrally extended, the quadrate being relatively curved, and the distal region of the ischial shaft being ventrally expanded, forming a large 'boot-like' process (Zhang et al. 2017a).

In lambeosaurines, the hypertrophied nasal passages associated with a wide variety of supracranial crests are entirely enclosed by the paired premaxillae and nasals (Ostrom 1962; Hopson 1975; Horner et al. 2004; Evans et al. 2009). In the original description, Young (1958) referred a partial left premaxilla, which only preserved the rostral portion, to IVPP V 725, the type of *Tsintaosaurus spinorhinus* (figure 8 in Young 1958). Therefore, the morphology of caudodorsal part of the premaxilla and the articular relationships between the premaxilla and nasal are ambiguous, and the rod-like nasal was considered as the whole cranial crest in most of the reconstructions. However, Prieto-Márquez and Wagner (2013) restored *Tsintaosaurus spinorhinus* with a hollow crest, which consists of premaxillae and nasals with the upturned prefrontals and frontals supporting caudoventrally (figures 7 and 8 in Prieto-Márquez and Wagner 2013), as in typical lambeosaurines, based on the skull characteristics and caudodorsal premaxillary fragments, IVPP V 829. We consider this new reconstruction would be more dependable, but our external observation and CT scan provide some new information about the nasal spine of *Tsintaosaurus spinorhinus*, as detailed below.

The main body of the nasal of *Tsintaosaurus spinorhinus*, the rod-like process, was initially described by Young (1958) as a hollow tubular structure, which were followed by the later authors (Buffettaut and Tong 1993, 1995; Prieto-Márquez and Wagner 2013), because it is impossible to observe the inside of the nasal in a conventional non-destructive way. However, Young (1958) did not find the ventral exit of the nasal tubular structure to the intracranial space, and in addition to this, Prieto-Márquez and Wagner (2013) also suspected that the nasal tubular structure was too narrow for air to pass through. Thus, they doubted that the nasal was not hollow, but they still reconstructed the nasal structure as a diverticulum, which is different from other lambeosaurines, because of lacking more evidence (Prieto-Márquez and Wagner 2013). As described above, our CT scan data show that the cross section of the rod-like process of nasal is a solid sandwich structure (Figure 3(j-q)), which consists of a dense medial part and two lateral less denser areas, rather than the hollow annular structure. The medial part is not surrounded by the two lateral ones, and its rostral margin delimits a rostral boundary of the sagittal ridge of the nasal. In addition, the caudal portion of the medial dense area is also touching the caudal border of nasal, particularly, especially in the caudoventral part of the nasal, the caudal margin of the medial area constitutes the caudodorsal surface and the contact surface for the frontal (Figure 3(n-q)). In the most part of the rod-like process, the medial denser area penetrates the rod-like process in the cross section, so the nasals could not enclose a hollow cavity to form a tube-like process. The medial denser area is interpreted as the internasal articulation extending through the whole distance of the nasal rostrocaudal, and the lateral lower density regions are interpreted as the paired nasal plates, which are close to the internasal articulation part without enclosing any space. We suspect that the difference in the density is probably caused by the fusion and reinforce of the nasal for supporting and transferring the weight from the crest, like denser and upturned prefrontal.

As the original description and reconstruction of Young (1958), the nasal spine of IVPP V 725 extended slightly rostrodorsally. We concur with this opinion, but we suggest that the nasal spine may be more inclined rostrally than the current appearance (Figure 4). Because, as the external description and CT scan revelation above, there is a significant fracture between the rod-like process and the block-like process of the nasal, and the fracture surfaces of these two parts are almost similar. If the two parts of the nasal fit together, the rod-like process would lean forward (Figure 4), because the position of the base of the nasal is more stable than the rod-like process. However, the nasal would not lean down and extend rostroventrally as in saurolophine hadrosaurids (Taquet 1991), since the upturned frontal and prefrontal in both the holotype (IVPP V 725) and paratype (IVPP V 818) indicate that *Tsintaosaurus spinorhinus* indeed has a dorsal-extended nasal spine. As our observation of holotype and paratype of *Tsintaosaurus spinorhinus*, the dorsal margin of the infratemporal fenestra lies approximately at the same level as the dorsal margin of the orbit, and the caudal region of the skull roof is subhorizontal relative to the frontal plane (Prieto-márquez 2010b: character 192), as in other basal lambeosaurines like *Aralosaurus tuberiferus* (Godefroit et al. 2004a) and *Jaxartosaurus aralensis* (Rozhdestvensky 1968). Thus, we reject the opinion of Prieto-Márquez and Wagner (2013) that the caudoventral sloping of the skull roof causes the nasal angled posteriorly.

As noted above, between the two caudal processes of the nasals in IVPP V 725, there is a narrow strip structure (Figure 3(c)), which Prieto-Márquez and Wagner (2013) regarded as the narrow

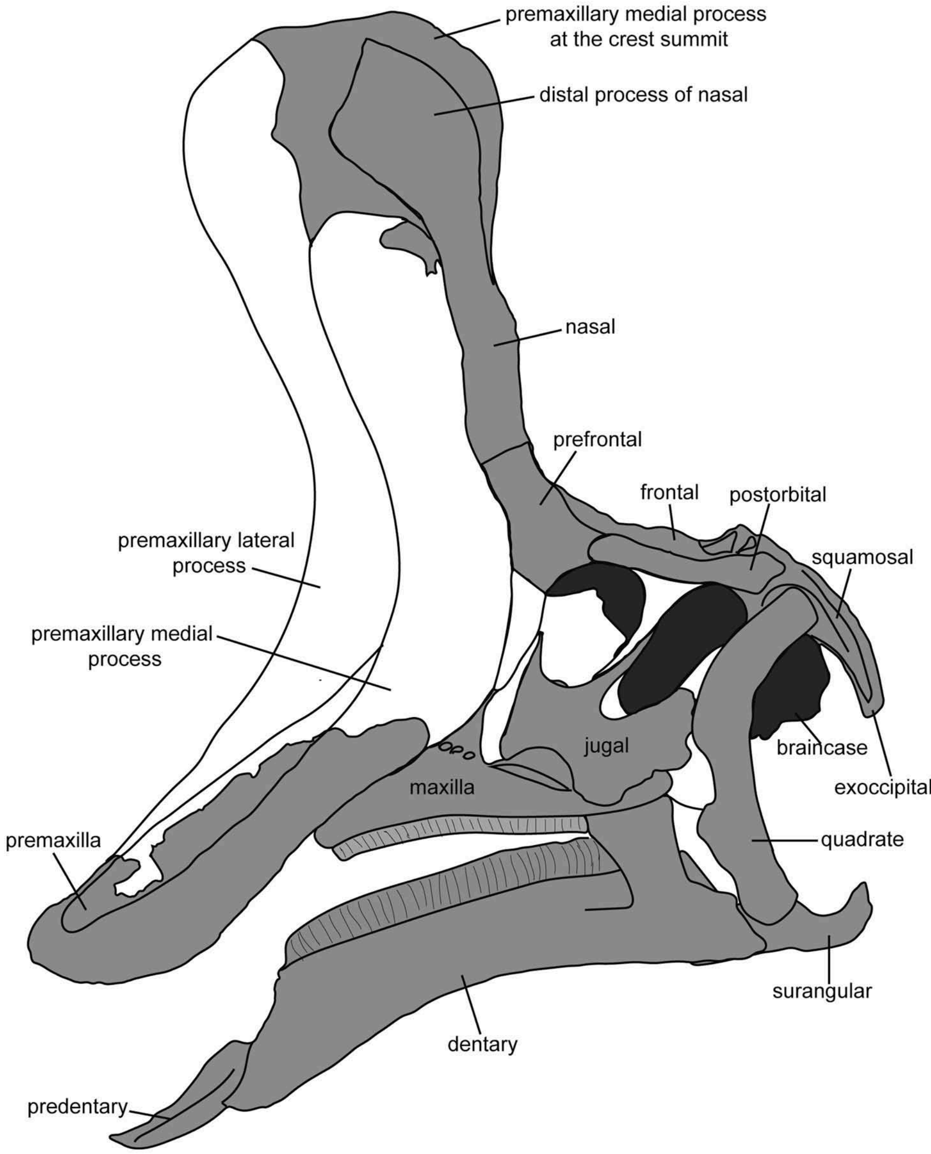

Figure 4. The reconstruction on the *Tsintaosaurus* skull. The grey areas indicate the available bones; the white areas are missing bones.

rostromedial process of frontal like in *Jaxartosaurus aralensis* (Rozhdestvensky 1968) and *Kazaklambia convincens* (Bell and Brink 2013). However, the above external description and CT scan on the morphology and articular relationships of this narrow strip structure and the surrounding nasals and frontals revealed another interpretation of this structure as a deep groove filled with sediment (Figure 2(c), 3(n-q)). Although the narrow strip structure in IVPP V 725 is not a perforative opening, it has a distinct boundary with nasal and frontal bones (Figure 2(c)). In addition, the border is also obvious in the CT scan imagery of the nasal crest of IVPP V 725 (Figure 3(n-q)). The material in this structure is different from the nasal and frontal, but same as in the nasal-frontal and interfrontal sutures. As the CT scan shows the sagittal section of the narrow strip structure is a semicircle, which is anastomose with the morphology of the deep cleft between the two nasal articulate surfaces of the frontals in IVPP V 818 (Figure 2(e)). This structure is more similar with the median hemispherical notch in rostral border of the frontal in *Amurosaurus*, which is derived from the frontal-nasal fontanelle as the described by Godefroit et al. (2004b). The frontal-nasal fontanelle, a central opening between the nasal and frontal bones, is present in non-hadrosaurid Hadrosauroidea (e.g. *Bactrosaurus, Levnesovia, Eotrachodon*), Saurolophinae (e.g. *Lophorhothon*, Edmontosaurus), and basal Lambeosaurinae (e.g. *Aralosaurus, Amurosaurus*) (Langston 1960; Rozhdestvensky 1966, 1968; Maryańska and Osmólska 1979; Godefroit et al. 2004a, 2004b; Sues and Averianov 2009; Prieto-Márquez et al. 2016). The presence of the frontal-nasal fontanelle is considered to be an ontogenetic character and responsible for the variability of crest structures, as essentially the same role of the premaxilla-nasal fontanelle in the derived Lambeosaurinae (Maryańska and Osmólska 1979; Godefroit et al. 2004a; Brink et al. 2011). As the CT scan revelation above, the narrow frontal-nasal groove of IVPP V 725 shrinks ventrally and almost closes at the bottom (Figure 3(n-q)), so this groove may not penetrate the entire skull roof as a fontanelle. However, the cleft between the paired nasal articulate surfaces of the frontals seems to open at the bottom in IVPP V 818, which is smaller than IVPP V 725, and would represent a younger individual. We suspect that there would be a frontal-nasal fontanelle at the skull roof of juvenile or sub-adult *Tsintaosaurus*. During the ontogeny, the bottom of the fontanelle is fused and ossified, and the fontanelle turned to a narrow groove between the frontal and nasal bones. The narrow groove may refer to the previous presence of the fontanelle during the earlier growth stages.

Conclusions

The CT scan reveals that the rod-like nasal spine of *Tsintaosaurus spinorhinus* is a solid sandwich structure, rather than a hollow tubular structure, and there are a series of breakages in the distal process. There is a significant fracture between the rod-like process and the block-like process of the nasal, and if we fit the two parts of nasal together, the nasal spine may be more inclined rostrally than the current appearance. The external description and CT scan show a narrow strip structure surrounded by nasals and frontals. This structure could be interpreted as a sediment-filled groove derived from the frontal-nasal fontanelle that possibly occurs in earlier growth stages. Our results are basically consistent with the reconstruction of the cranial crest of *Tsintaosaurus spinorhinus* by Prieto-Márquez and Wagner (2013) and provide some new information about the nasal spine of *Tsintaosaurus spinorhinus*.

Acknowledgments

We thank Long Xiang (IVPP) for specimen preparation, Jie Zhang (IVPP) for photos, as well as Shusen Zhao and Yemao Hou (IVPP) for CT scan.

Disclosure statement

No potential conflict of interest was reported by the authors.

Funding

This study was supported by the National Natural Science Foundation of China (41172018, 41688103, 41572020), the Strategic Priority Research Program (B) of the CAS (XDB18000000), the Laiyang Cretaceous Fauna Research Program of the China University of Geosciences, Beijing (H02657), and the Laiyang Government Cooperation Dinosaur Project.

References

An W, Kuang H-W, Liu YQ, Peng N, Xu KM, Xu H, Zhang P, Wang KB, Chen SQ, Zhang YX. 2016. Detrital zircon dating and tracing the provenance of dinosaur bone beds from the Late Cretaceous Wangshi Group in Zhucheng, Shandong, East China. J Palaeogeogr. 5(1):72–99.

Becerra M, Paulina-Carabajal A, Cruzado-Caballero P, Taborda J. 2018. First endocranial description of a South American hadrosaurid: the neuroanatomy of *Secernosaurus koerneri* from the Late Cretaceous of Argentina. Acta Palaeontol Pol. 63(4):693–702.

Bell PR, Brink KS. 2013. *Kazaklambia convincens comb. nov*., a primitive juvenile lambeosaurine from the Santonian of Kazakhstan. Cretaceous Res. 45:265–274.

Bell PR, Snively E, Shychoski L. 2009. A comparison of the jaw mechanics in hadrosaurid and ceratopsid dinosaurs using finite element analysis. Anat Rec. 292(9):1338–1351.

Bolotsky YL, Kurzanov S. 1991. The hadrosaurs of the Amur region. In: Moiseyenko VG, editor. Geology of the Pacific ocean border. Blagoveschensk: Amur KNII; p. 94–103. Russian.

Brett-Surman MK 1989. A revision of the Hadrosauridae (Reptilia: Ornithischia) and their evolution during the Campanian and Maastrichtian [dissertation]. Washington (DC): George Washington University.

Brink KS, Zelenitsky DK, Evans DC, Therrien F, Horner HR. 2011. A sub-adult skull of *Hypacrosaurus stebingeri* (Ornithischia: lambeosaurinae): anatomy and comparison. Hist Biol. 23(01):63–72.

Buffetaut E, Tong H. 1993. *Tsintaosaurus spinorhinus* Young and *Tanius sinensis* Wiman: a preliminary comparative study of two hadrosaurs (Dinosauria) from the Upper Cretaceous of China. C.R. Acad Sci Ser II. 317(9):1255–1261.

Buffetaut E, Tong H. 1995. The Late Cretaceous dinosaurs of Shandong, China: old finds and new interpretations. In: Sun AL, Wang YQ, editors. Sixth symposium on mesozoic terrestrial ecosystems and biota. Beijing: China Ocean Press; p. 139–142.

Cruzado-Caballero P, Fortuny J, Llacer S, Canudo JI. 2015. Paleoneuroanatomy of the European lambeosaurine dinosaur *Arenysaurus ardevoli*. PeerJ. 3:e802.

Dong ZM. 1978. New genus of Pachycephalosauria from Laiyang, Shantung. Vertebr PalAsiat. 16(4):225–228.

Evans DC. 2006. Nasal cavity homologies and cranial crest function in lambeosaurine dinosaurs. Paleobiology. 32(1):109–125.

Evans DC, Ridgely R, Witmer LM. 2009. Endocranial anatomy of lambeosaurine hadrosaurids (Dinosauria: ornithischia): a sensorineural perspective on cranial crest function. Anat Rec. 292(9):1315–1337.

Farke AA, Chok DJ, Herrero A, Scolieri B, Werning S. 2013. Ontogeny in the tube-crested dinosaur *Parasaurolophus* (Hadrosauridae) and heterochrony in hadrosaurids. PeerJ. 1:e182.

Godefroit P, Alifanov V, Bolotsky Y. 2004a. A re-appraisal of *Aralosaurus tuberiferus* (Dinosauria, Hadrosauridae) from the Late Cretaceous of Kazakhstan. Bull Inst R Sci Nat Belg Sci Terre. 74:139–154.

Godefroit P, Bolotsky Y, Alifanov V. 2003. A remarkable hollow-crested hadrosaur from Russia: an Asian origin for lambeosaurines. C.R. Palevol. 2 (2):143–151.

Godefroit P, Bolotsky YL, Lauters P. 2012. A new saurolophine dinosaur from the latest Cretaceous of far eastern Russia. PLoS One. 7(5):e36849.

Godefroit P, Bolotsky YL, Van Itterbeeck J. 2004b. The lambeosaurine dinosaur *Amurosaurus riabinini*, from the Maastrichtian of Far Eastern Russia. Acta Palaeontol Pol. 49(4):585–618.

Godefroit P, Shulin H, Tingxiang Y, Lauters P. 2008. New hadrosaurid dinosaurs from the uppermost Cretaceous of northeastern China. Acta Palaeontol Pol. 53(1):47–75.

Godefroit P, Zan S, Jin L. 2000. *Charonosaurus jiayinensis ng, n. sp*., a lambeosaurine dinosaur from the Late Maastrichtian of northeastern China. C.R. Acad Sci Ser IIa. 330(12):875–882.

Hopson JA. 1975. The evolution of cranial display structures in hadrosaurian dinosaurs. Paleobiology. 1(1):21–43.

Horner HR, Weishampel DB. 1990. Hadrosauridae. In: Weishampel DB, Dodson P, Osmolska H, editors. The dinosauria. Berkeley: University of California Press; p. 534–561.

Horner HR, Weishampel DB, Forster CA. 2004. Hadrosauridae. In: Weishampel DB, Dodson P, Osmolska H, editors. The dinosauria. 2nd ed. Berkeley: University of California Press; p. 438–463.

Hu CZ. 1973. A new hadrosaur from the Cretaceous of Chucheng, Shantung. Acta Geol Sin. 2:179–202.

Langston W. 1960. The vertebrate fauna of the Selma Formation of Alabama, Part 6: the Dinosaurs. Fieldiana: Geol Mem. 3:313–361.

Lauters P, Vercauteren M, Bolotsky YL, Godefroit P, Butler RJ. 2013. Cranial endocast of the lambeosaurine hadrosaurid *Amurosaurus riabinini* from the Amur Region, Russia. PLoS One. 8(11):e78899.

Liu Y, Kuang HW, Peng N, Ji S, Wang XL, Chen SS, Zhang Y, Xu H. 2010. Sedimentary facies and taphonomy of Late Cretaceous deaths of dinosaur, Zhucheng, eastern Shandong. Geol Rev. 56:457–468.

Lund EK, Gates TA. 2006. A historical and biogeographical examination of hadrosaurian dinosaurs. New Mex Mus Nat Hist Sci Bull. 35:263–276.

Maryańska T, Osmólska H. 1979. Aspects of hadrosaurian cranial anatomy. Lethaia. 12(3):265–273.

Maryańska T, Osmólska H. 1981. Cranial anatomy of *Saurolophus angustirostris* with comments on the Asian Hadrosauridae (Dinosauria). Palaeontol Pol. 42:5–24.

Nagao T. 1936. *Nipponosaurus sachalinensis*: a new genus and species of trachodont dinosaur from Japanese Saghalien. J Fac Sci Hokkaido Imp Univ 4 Geol Mineral. 3(2):185–220.

Ostrom JH. 1962. The cranial crests of hadrosaurian dinosaurs. Postilla. 62:1–29.

Poropat SF, Kear BP. 2013. Reassessment of coelurosaurian (Dinosauria, Theropoda) remains from the Upper Cretaceous Wangshi Group of Shandong Province, China. Cretaceous Res. 45:103–113.

Prieto-márquez A. 2010a. Global phylogeny of Hadrosauridae (Dinosauria: ornithopoda) using parsimony and Bayesian methods. Zool J Linn Soc. 159 (2):435–502.

Prieto-márquez A. 2010b. Global historical biogeography of hadrosaurid dinosaurs. Zool J Linn Soc. 159(2):503–525.

Prieto-Márquez A, Erickson GM, Ebersole JA. 2016. Anatomy and osteohistology of the basal hadrosaurid dinosaur *Eotrachodon* from the uppermost Santonian (Cretaceous) of southern Appalachia. PeerJ. 4:e1872.

Prieto-Márquez A, Wagner JR. 2013. The 'unicorn'dinosaur that wasn't: a new reconstruction of the crest of *Tsintaosaurus* and the early evolution of the lambeosaurine crest and rostrum. PLoS One. 8(11):e82268.

Ramírez-Velasco AA, Morales-Salinas E, Hernández-Rivera R, Tanke DH. 2017. Spinal and rib osteopathy in *Huehuecanauhtlus tiquichensis* (Ornithopoda:

hadrosauroidea) from the Late Cretaceous in Mexico. Hist Biol. 29 (2):208–222.

Riabinin AN. 1938. Some results of the study of the Upper Cretaceous dinosaurian fauna from the vicinity of the station SaryAgach, South Kazakhstan. Probl Palaeontol. 4:130–136. Russian.

Rozhdestvensky AK. 1966. New Iguanodonts from Central Asia: phylogenetic and taxonomic interrelationships of late Iguanodontidae and early Hadrosauridae. Paleontol J. 1966(3):103–116.

Rozhdestvensky AK. 1968. Hadrosaurs of Kazakhstan. In: Tatarinov LP, editor. Upper paleozoic and mesozoic amphibians and reptiles. Moscow: Akademia Nauk S.S.S.R.; p. 97–141. Russian.

Rozhdestvensky AK. 1977. The study of dinosaurs in Asia. J Palaeontol Soc India. 20:102–119.

Sues HD, Averianov A. 2009. A new basal hadrosauroid dinosaur from the Late Cretaceous of Uzbekistan and the early radiation of duck-billed dinosaurs. Proc R Soc London B. 276(1667):2549–2555.

Sullivan RM, Williamson TE. 1999. A new skull of *Parasaurolophus* (Dinosauria: hadrosauridae) from the Kirtland Formation of New Mexico and a revision of the genus. New Mex Mus Nat Hist Sci Bull. 15:1–52.

Taquet P. 1991. The status of *Tsintaosaurus spinorhinus* Young, 1958 (Dinosauria). In: Kielan-Jaworowska Z, Heintz N, Nakrem HA, editors. Fifth Symposium of Mesozoic terrestrial ecosystems and biota. Oslo: Contributions from the Paleontological Museum; p. 63–64.

Wang XL, Wang Q, Wang JH, Zhang JL, Cheng X, Jiang SX, Pan R. 2010. An overview on the Cretaceous dinosaurs and their eggs from Laiyang, Shandong Province, China. In: Dong W, editor. Proceedings of the twelfth annual meeting of the chinese society of vertebrate paleontology. Beijing: China Ocean Press; p. 293–316.

Wiman C. 1929. Die Kreide-Dinosaurier aus Shantung. Palaeontol Sin C. 6:1–67.

Xing H, Zhao X, Wang K, Li D, Chen S, Mallon JC, Zhang Y, Xu X. 2014. Comparative osteology and phylogenetic relationship of *Edmontosaurus* and *Shantungosaurus* (Dinosauria: hadrosauridae) from the Upper Cretaceous of North America and East Asia. Acta Geol Sin. 88(6):1623–1652. (English Edition).

Yan J, Chen JF. 2005. Clinopyroxene megacrysts in the Late Mesozoic basalts from Daxizhuang, Jiaozhou. J Anhui Univ Sci Technol Nat Sci. 25:9–20.

Young CC. 1958. The dinosaurian remains of Laiyang, Shantung. Palaeontol Sin. 16:1–138.

Zhang JL, Wang Q, Jiang SX, Cheng X, Li N, Qiu R, Zhang X, Wang X. 2017a. Review of historical and current research on the Late Cretaceous dinosaurs and dinosaur eggs from Laiyang, Shandong. Vertebr PalAsiat. 55:187–199.

Zhang JL, Wang XL, Wang Q, Jiang SX, Cheng X, Li N, Qiu R. 2017b. A new saurolophine hadrosaurid (Dinosauria: ornithopoda) from the Upper Cretaceous of Shandong, China. An Acad Bras Cienc. 91(supl.2):1–19.

Zhang YG, Wang KB, Chen SQ, Liu D, Xing H. 2019. Osteological re-assessment and taxonomic revision of "*Tanius laiyangensis*"(Ornithischia: hadrosauroidea) from the Upper Cretaceous of Shandong, China. The Anat Rec. doi:10.1002/ar.24097 (online).

Zhen SN. 1976. A new species of hadrosaur from Shandong. Vertebr PalAsiat. 14 (3):166–168.